A simple, reliable and robust reinforcement method for the fabrication of (RE)–Ba–Cu–O bulk superconductors

Devendra K Namburi[iD]**, Kaiyuan Huang**[iD]**, Wayne Lau, Yunhua Shi**[iD]**, Kysen G Palmer, Anthony R Dennis, David A Cardwell**[iD] **and John H Durrell**[iD]

Department of Engineering, University of Cambridge, Cambridge CB2 1PZ, United Kingdom

E-mail: dkn23@cam.ac.uk

Abstract

Bulk high temperature superconductors (HTS) based on the rare-earth barium cuprates [(RE)BCO] have the potential to be applied in a variety of engineering and technological applications such as trapped field magnets, rotating electrical machines, magnetic bearings and flywheel energy storage systems. The key materials figure of merit for most practical applications of bulk superconductors is simply the product of the maximum current density that can be supported, which correlates directly with the maximum achievable trapped magnetic field, and the physical length scale over which the current flows. Unfortunately, however, bulk (RE)BCO superconductors exhibit relatively poor mechanical properties due to their inherent ceramic nature. Consequently, the performance of these materials as trapped field magnets is limited significantly by their tensile strength, rather than critical current and size, given that the relatively large Lorentz forces produced in the generation of large magnetic fields can lead to catastrophic mechanical failure. In the present work, we describe a simple, but effective and reliable reinforcement methodology to enhance the mechanical properties of (RE) BCO bulk superconductors by incorporating hybrid SiC fibres consisting of a tungsten core with SiC cladding within the bulk microstructure. An improvement in tensile strength by up to 40% has been achieved via this process and, significantly, without compromising the superconducting performance of the bulk material.

Keywords: bulk superconductor, reinforcement, mechanical property, high field trapped field, SiC hybrid fibre, tensile strength, top seeded melt growth

(Some figures may appear in colour only in the online journal)

1. Introduction

Bulk high temperature superconductors (HTS) based on the rare-earth barium cuprates [(RE)BCO] and consisting of a continuous, $(RE)Ba_2Cu_3O_{7-\delta}$ (RE-123) superconducting phase matrix containing embedded non-superconducting $(RE)_2BaCuO_5$ (RE-211) particle inclusions fabricated in the form of large single grains can be used as pseudo permanent magnets with trapped fields of up to an order of magnitude higher than those possible with conventional permanent magnets [1, 2]. In general, the trapped field achievable in a bulk superconductor is proportional to the $J_c{}^* d$ product, where J_c is the critical current density and d is the size of the single grain [3]. Such bulk trapped field magnets are potentially useful for a wide variety of engineering applications including trapped field magnets, rotating electrical machines, flywheel energy storage systems, magnetic separators, fault current limiters and magnetic bearings [4, 5].

Top seeded melt growth (TSMG) is a well-established processing technique for the fabrication of single grain (RE)
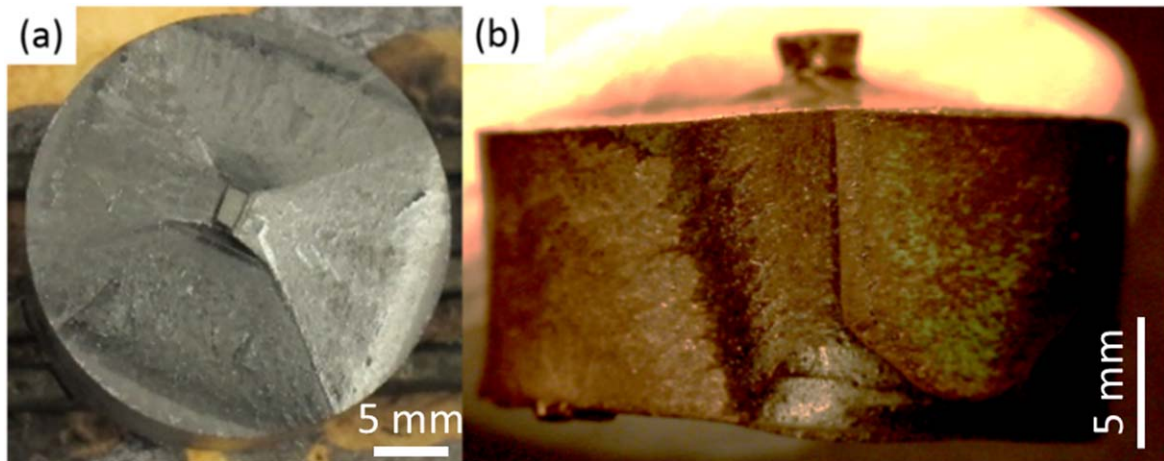
Figure 1. (a) Facet lines along the a–b plane and (b) and *c*-axis as observed in a YBCO single grain sample fabricated via the top seeded melt growth (TSMG) technique.
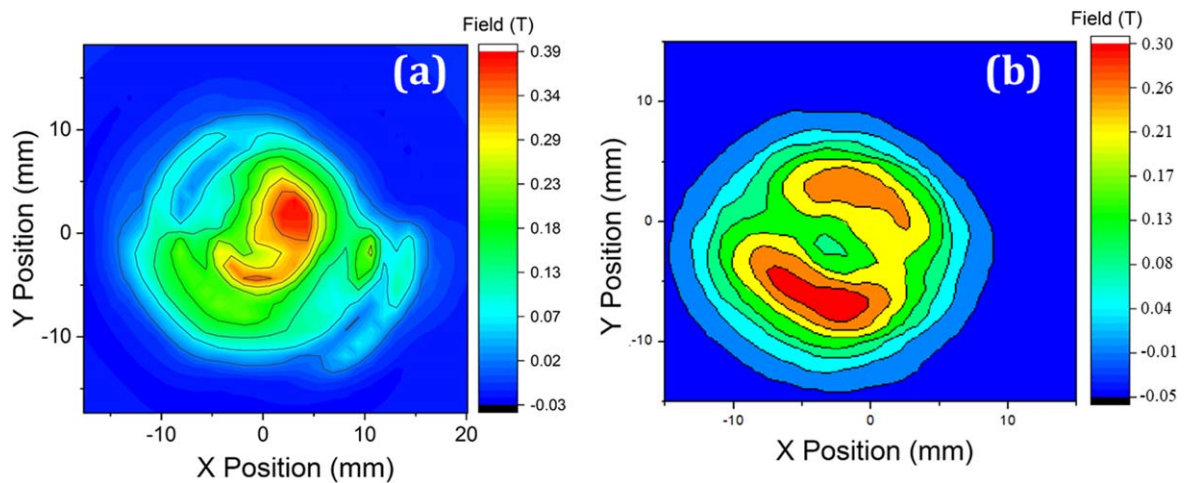

Figure 2. Trapped field profile measured at 77 K for a YBCO sample that cracked either (a) partially or (b) completely, in previous experiments in which they were exposed to very large magnetic fields of 18 T. The cracks were not visible on optical examination.

BCO monoliths of up to 10 cm in diameter [6–8]. TSMG involves placing a seed crystal [with a peritectic temperature 'T_p' greater than that of the (RE)BCO material being grown] at the centre of the top surface a compacted green pellet formed, typically, from 75 wt% RE-123 and 25 wt% RE-211. The precursor pellet and seed is then subjected to a controlled heating profile whereby the arrangement is heated initially above T_p of the target RE-123 phase and, subsequently, cooled slowly back through T_p. This leads to grain nucleation and subsequent recrystallisation from the seed crystal as the peritectic reaction proceeds throughout the bulk sample. The resultant single grain typically exhibits characteristic, four-fold growth-facet lines both in the *a–b* plane and along the *c*-axis, as shown in figures 1(a) and (b) respectively.

The superconducting performance of bulk (RE)BCO materials continues to improve. A 65 mm diameter GdBCO-Ag bulk sample has been reported to trap a magnetic field of 3 T at 77 K [9]. Nano-sized $(RE)_2Ba_4CuMO_y$ (RE-2411) inclusions when added to the RE-123 phase matrix enabled material to support a current density in excess of 100 kA cm^{-2}, at 77 K [10]. Additionally similar performance in current

density has been observed in mixed RE systems with source of flux pinning arising from lattice mismatch effects [11]. Trapped fields in excess of 17 T at 26 K can also be achieved via suitable post-melt-processing reinforcement techniques, such as those based on resin-impregnated carbon-fibre [12] and shrink-fitted stainless steel [13].

It is important to note that the limiting factor of high trapped field performance in these materials is their tensile strength, rather than simply the critical current density a single grain can support. The Lorentz forces generated during sample charging at a field of 15 T can create a hoop stress greater than 100 MPa [14]. As a result, without reinforcement bulk superconductors typically cannot withstand magnetic fields larger than 7–8 T [15, 16]. The material failure method for this type of loading is via the propagation of large cracks throughout the single grain microstructure [17]. Figure 2 shows trapped field profiles measured at 77 K for YBCO samples that had been subjected in previous experiments to a large magnetic field of 18 T. It is apparent that mechanical failure has essentially destroyed the integrity of sample, resulting in a non-conical trapped field profile.
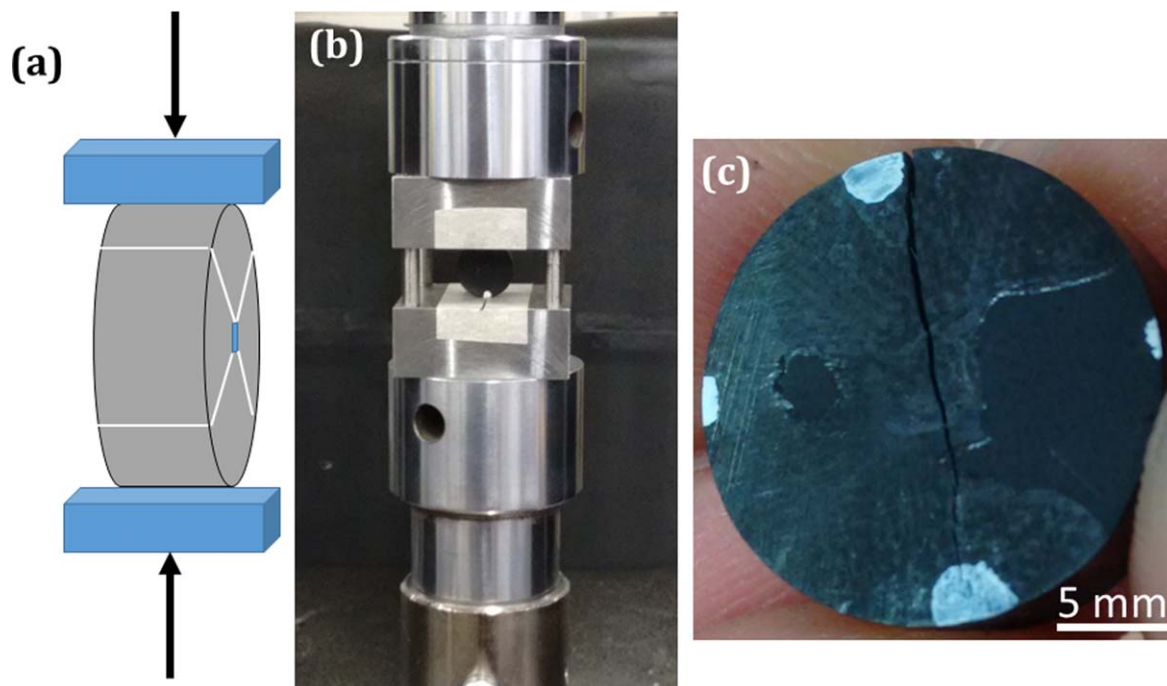
Figure 3. (a) Schematic diagram showing the application of compressive force parallel to growth sector direction for the YBCO samples. (b) An image captured during the mechanical tensile strength test of a YBCO sample performed by the Brazilian technique. The crack formed in the sample during the fracture process is shown in (c).

Efforts have been made to improve the mechanical strength of single grain (RE)BCO materials to enable larger magnetic fields to be trapped. The addition of silver (whose melting point is lower than the T_p of (RE)BCO, overcoming the problems of unwanted nucleation and the formation of sub-grains) has helped significantly to improve the mechanical strength of the (RE)BCO RE-123/RE-211 composite. The Ag particles partially fill the pores and cracks present in the microstructure of these materials and thereby prevent crack initiation and propagation to some extent when exposed to large magnetic fields [18–20].

The incorporation of reinforcing fibres in conventional ceramics is a well-established route to enhance the properties of these highly brittle materials. The use of both oxide and non-oxide fibres has been investigated in conventional ceramics specifically for this purpose. In particular, recent work has showed that it is possible to achieve significant improvement in terms of mechanical strength and stability (both chemical and thermal) by reinforcing ceramics with both SiC and carbon nanotubes [21–25]. We extend this approach in the present work to the processing of (RE)BCO bulk superconductors. The challenge in this case, in contrast to non-functional ceramics, is the incorporation of mechanical reinforcement without compromising the superconducting properties of the parent single grain.

2. Experimental

Single grain, YBCO bulk superconductors of diameter 16 mm, 20 mm and 25 mm containing fibres were fabricated by the top seeded melt growth (TSMG) technique. The fibres studied in the present work were of three types: (i) metallic tungsten (W), (ii) SiC and (iii) hybrid fibres consisting of SiC-clad tungsten cores. Precursor powder comprising 75 wt% Y-123 + 25 wt% Y-211 + 0.5 wt% CeO_2 was used to prepare the single grain YBCO samples. Y-123 and Y-211 powders, each of 99.9% purity, were procured from Toshima Manufacturing Co. Ltd, Japan and CeO_2 of 99.9% purity was purchased from Sigma Aldrich. All the fibres studied in the present work were procured from American Elements, USA and were introduced into the precursor powder processing during the compaction stage, either in a mixed form or in the configurations outlined in section 3. Samples with no added fibres were also prepared under similar conditions for each sample set to provide an experimental control test specimen.

The effect of the addition of fibres on the T_p of mixed precursor powder (comprising of 75 wt% Y-123 + 25 wt% Y-211 + 0.5 wt% CeO_2 + fibres) was investigated by thermogravimetry/differential thermal analysis (TG-DTA) under air up to temperatures of 1200 °C with heating and cooling rates of 10 °C per minute. The uniaxially-pressed pellets were capped with a buffer pellet of diameter 5 mm composed of 75 wt% Y-123 + 25 wt% Y-211, with a NdBCO or generic seed crystal [26, 27], which was placed on the top of the buffer pellet to complete the arrangement. The entire assembly was then melt processed using a standard heat profile described elsewhere [28]. Typically, the heat treatment comprised of heating the sample assembly in a box furnace to a temperature of 1055 °C (i.e. above the T_p of Y-123 phase to promote the incongruent melting of Y-123 phase to form solid Y-211 and copper-rich liquid phase $BaCuO_2$ and CuO).
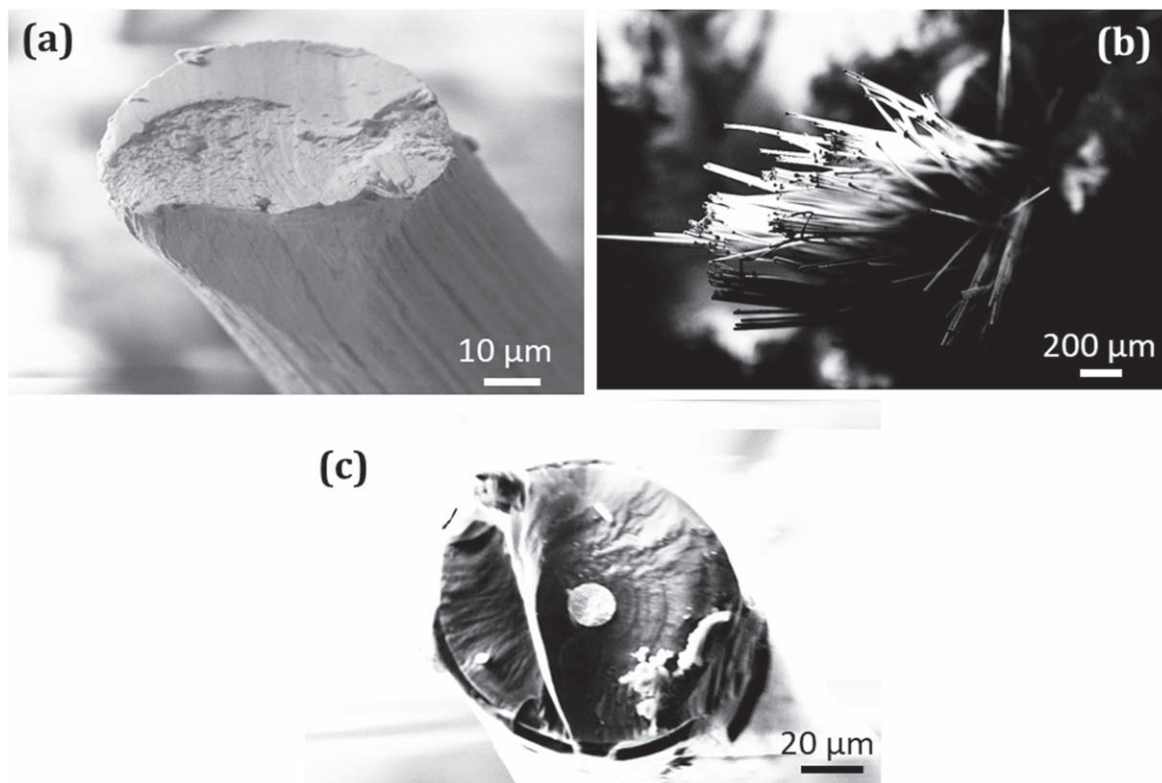
Figure 4. Scanning electron micrographs of (a) a W-metal fibre, (b) a multi-filamentary SiC fibre and (c) the cross-section of a SiC fibre monofilament with a W-core.

The sample assembly was then cooled slowly at a rate of 0.5 °C–0.7 °C/h through the T_p of the compound to 980 °C and then furnace cooled to room temperature. This heat treatment enabled the nucleation and growth of a YBCO single grain. The as-grown samples were subsequently oxygenated in a tube furnace at a temperature of 450 °C under oxygen gas flowing at a rate of 100 ml min^{-1}. The oxygenation process was carried out for 150 h to completely transform the tetragonal, non-superconducting Y-123 phase to the orthorhombic, superconducting phase.

In order to measure the ability of the samples to trap magnetic field, their top and bottom surfaces were each polished to obtain flat faces prior to field-cooling using liquid nitrogen (77 K) in an applied magnetic field of 1.4 T. The field was then removed and the trapped magnetic field in the sample was measured by a scanning array of Hall probes consisting of 19 Hall probes (procured from Lakeshore). A DC current of ±1 mA was passed through the Hall sensors, which were connected in series, using a programmable current source (Keithley, 220) and Hall voltage across each of these probes was measured using a Digital multimeter (Agilent, 34401 A). A Keithley 7001 switch box was used to toggle between the Hall probe point to be measured. All the data were acquired using LabVIEW. The measured Hall probe voltages were converted into field values and a temperature correction for operation at 77 K was performed. Data were plotted in Origin to obtain 3D contour maps and 2D surface profile plots. Further details of the Hall probe scanning system can be found elsewhere [29]. The mechanical tensile strength of the YBCO bulk superconductors melt processed with and without fibres was measured by the Brazilian technique [30–32]. The circumferential surface of the oxygenated samples was polished for each of the samples in order to remove any inhomogeneities. The samples were then subjected to a mechanical test by applying a compressive force parallel to the different growth sector directions, as shown in figures 3(a) and (b), in a tensile testing machine (Instron, model 5584) until a hairline crack formed (as shown in figure 3(c)) along the principal axis as a result of induced tensile stress in the direction perpendicular to that of the applied force.

The indirect tensile strength, σ, of the single grain samples was calculated from $\sigma = \frac{2P}{\pi d t}$, where P is the applied load on the sample at fracture, and d and t are the diameter and thickness of the sample, respectively. The samples were sliced using a diamond saw and polished down to a micron-level finish using grinding foils and a colloidal suspension containing diamond particles. The microstructure of the fractured or polished sample surfaces at every stage of preparation was observed using either a scanning electron microscope (with an EDX facility) or an optical microscope equipped with a polarizer. The compositions of the fibres were analysed using the EDX spectrometer installed in the scanning electron microscope.

Table 1. Characteristics of the fibres used in the present work.

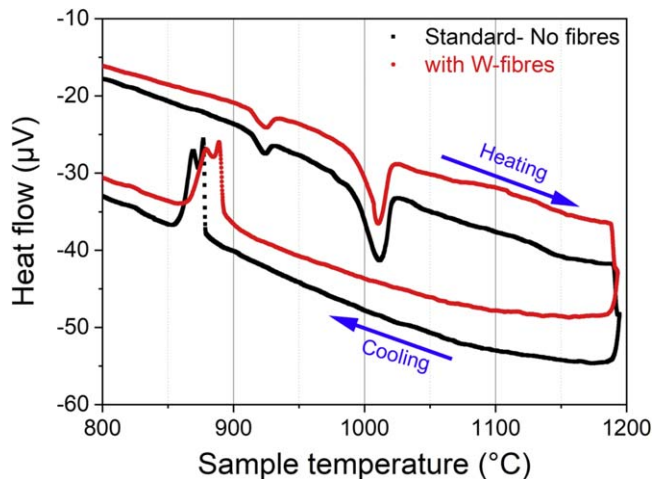| Fibre-type	Diameter	Melting point	Remarks
W-metal fibre	50 μm	3410 °C	Tensile strength: 750 MPa
Multi-filamentary SiC fibre	1.5 μm	2730 °C	Stack of 500 fibres
Monofilament SiC hybrid fibre	100 μm	Not provided	W in the core and SiC working as clad

Figure 5. Thermal scans obtained from precursor powder of composition 75 wt% Y-123 + 25 wt% Y-211 + 0.5 wt% CeO$_2$, with and without W-fibres. The curves in red (on-line version) and black correspond to powders with and without the W-fibres, respectively. These data indicate that the addition of W-fibres to the precursor powder does not affect the peritectic temperature T_p of YBCO significantly.

3. Results and discussion

Electron micrographs of the fibres employed in the present work i.e. W-metal, multi-filamentary SiC and monofilamentary hybrid SiC with a W-core, are shown in figures 4(a)–(c) respectively. It can be seen from figure 4(c) that the mono-filament SiC fibre is ~100 μm in diameter with a tungsten core of diameter ~15 μm. The presence of these fibres in the microstructure of the bulk superconductor was confirmed via EDX analysis. Further details of the fibres are summarised in table 1.

YBCO single grain bulk superconductors processed with and without fibres for each sample set were fabricated in the form of single grains by the buffer-aided, TSMG technique, as discussed further in sections 3.1–3.3.

3.1. Tungsten fibre reinforced YBCO

Tungsten fibres of diameter 50 μm were chopped into lengths of 1–4 mm and mixed with YBCO precursor powder containing 75 wt% Y-123 + 25 wt% Y-211 + 0.5 wt% CeO$_2$, using an agate mortar and pestle for 1 h. The precursor powders with and without added W-fibres were analysed by TG-DTA, as shown in figure 5, which confirms that the addition of W-fibres has not affected significantly the T_p of the powder (a reduction of T_p by only 1 °C is observed compared to the standard powder sample).

The sintered powder containing W-fibres was pressed uniaxially into a pellet of 25 mm in diameter using a steel die. A NdBCO seed crystal was used to process the assembly into a single grain employing TSMG, as shown in figure 6. These samples were subsequently oxygenated and their super-conducting and mechanical properties measured. The trapped field measured for YBCO samples fabricated both with and without W-fibres at 77 K are shown in figure 7. It can be seen that the field trapping ability of the sample is enhanced slightly due to the presence of W-fibres.

A detailed microstructural study was carried out in order to understand the likely reasons for the enhanced trapped field properties of the sample containing W-fibres compared to the standard composition. YBCO samples containing W-fibre were polished and examined using a scanning electron microscope were observed to contain Y$_2$Ba$_4$Cu$_1$W$_1$O$_y$ (Y-2411) phase inclusions, as can be seen in figure 8, the presence of which is known to enhance flux pinning in bulk (RE)BCO, and hence trapped field and the field dependence of J_c [33]. Corresponding EDX data and element analysis are provided in figures 8(c) and (d).

The mechanical strength of the samples processed with and without W-fibres was measured by the Brazilian technique, which involved applying a compressive load to each test specimen until it fractured. Tensile strength plots for both the samples (i.e. the standard YBCO and YBCO containing W-fibres) are shown in figure 9. Although the super-conducting properties of the bulk single grains are improved by the addition of W-fibres, their mechanical properties are observed to deteriorate, as can be seen in the figure. The reason for this deterioration is due to the complete reaction of the W-fibres with the aggressive liquid phase (comprising of BaCuO$_2$ and CuO) during peritectic decomposition to form the Y-2411 phase. This undermines the motivation for adding fibres to the bulk (RE)BCO single grain (i.e. to improve mechanical strength), which necessitated an investigation of alternative fibre additives with better phase stability in the presence of the Ba–Cu–O liquid phase. As a result, reinforcement of YBCO with SiC fibres was explored, as discussed in the following sections.

3.2. Multi-filamentary SiC-fibre reinforced YBCO

Silicon carbide (SiC) is a promising candidate for reinforcing (RE)BCO bulk superconductors due to its superior thermo-mechanical properties and its stability both in terms of che-mical inertness (i.e. with the Ba–Cu–O liquid phase) and improved thermal stability. Higher melting temperature, high hardness, and low thermal expansion coefficient are other practical and desirable properties for this application of SiC.

Figure 6. Single grain YBCO samples containing added W-fibres fabricated by the top-seeded melt growth technique.
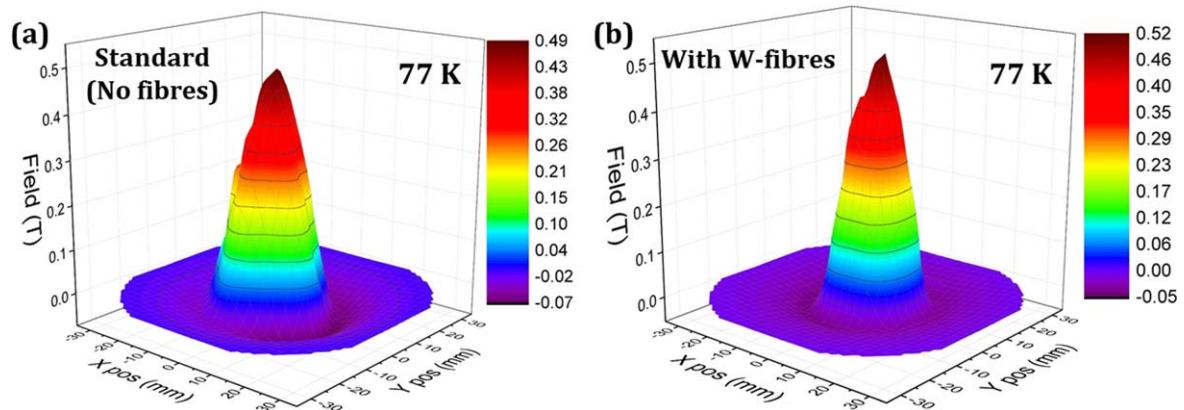

Figure 7. Trapped field measured at 77 K in (a) the reference YBCO sample of standard composition and (b) YBCO containing 1 wt% W-fibres.

A stack of 500 multi-filamentary SiC fibres, with a fibre diameter of $\sim$1.5 μm, were introduced into pressed YBCO compacts in two different configurations:

(i) The mixing of multifilamentary SiC fibres with the YBCO precursor powder followed by calcination and subsequent single grain growth of samples using a buffer-assisted TSMG technique to yield a random orientation of fibres;

(ii) The introduction of aligned, multifilamentary SiC fibres of the required length at the centre of the preform compact.

3.2.1. Configuration 1: random orientation of fibres. In the first configuration, the multifilamentary SiC fibres were chopped into lengths of 1–4 mm and mixed with YBCO precursor powder in the following composition; 75 wt% Y-123 + 25 wt% Y-211 + 0.5% CeO_2 + X wt% SiC fibre ($X = 0$, 0.25, 0.5 and 1). The mixture was calcined subsequently at 900 °C for 2 hours. DTA scans obtained from the mixed and calcined YBCO precursor powders with and without 0.25 wt% SiC fibres, are shown in figure 10.

The mixed YBCO powder containing dispersed multi-filamentary SiC-fibres (accounting for 0.25 wt%), was pressed unixially into a pellet as shown in figure 11(a) and capped with a buffer pellet and a NdBCO seed crystal. The entire sample assembly was then heated in a box furnace and melt processed using the buffer-assisted TSMG technique. This resulted in the growth of a single grain sample of diameter $\sim$20 mm, as shown in figure 11(b).

The trapped field measured in the YBCO sample containing 0.25 wt% SiC fibres is shown in figure 11(c). Despite the presence of high melting point SiC fibres, the sample grew successfully into a single grain, as evidenced by the clear 4-fold facet lines evident in figure 11(b) and the single peak in the trapped field measurements (figure 11(c)). The mechanical tensile strength in the SiC fibre-reinforced YBCO sample measured by the Brazilian technique is shown in figure 12. It can be seen that the addition and dispersion of SiC fibres in the precursor powder retains both mechanical strength and super-conducting performance, which is promising compared to that of a situation with reinforcement from W-fibres (figure 9).

3.2.2. Configuration 2: a–b plane aligned fibres. In the second configuration, the multifilamentary SiC fibres were chopped to lengths of $\sim$20 mm and were aligned at the center of the preform compact, as shown in figure 13(a). The sample assemblies prepared containing the multifilamentary SiC fibres are shown in figure 13(b). Despite of the presence of a relatively thick stack of SiC fibres at the center of the
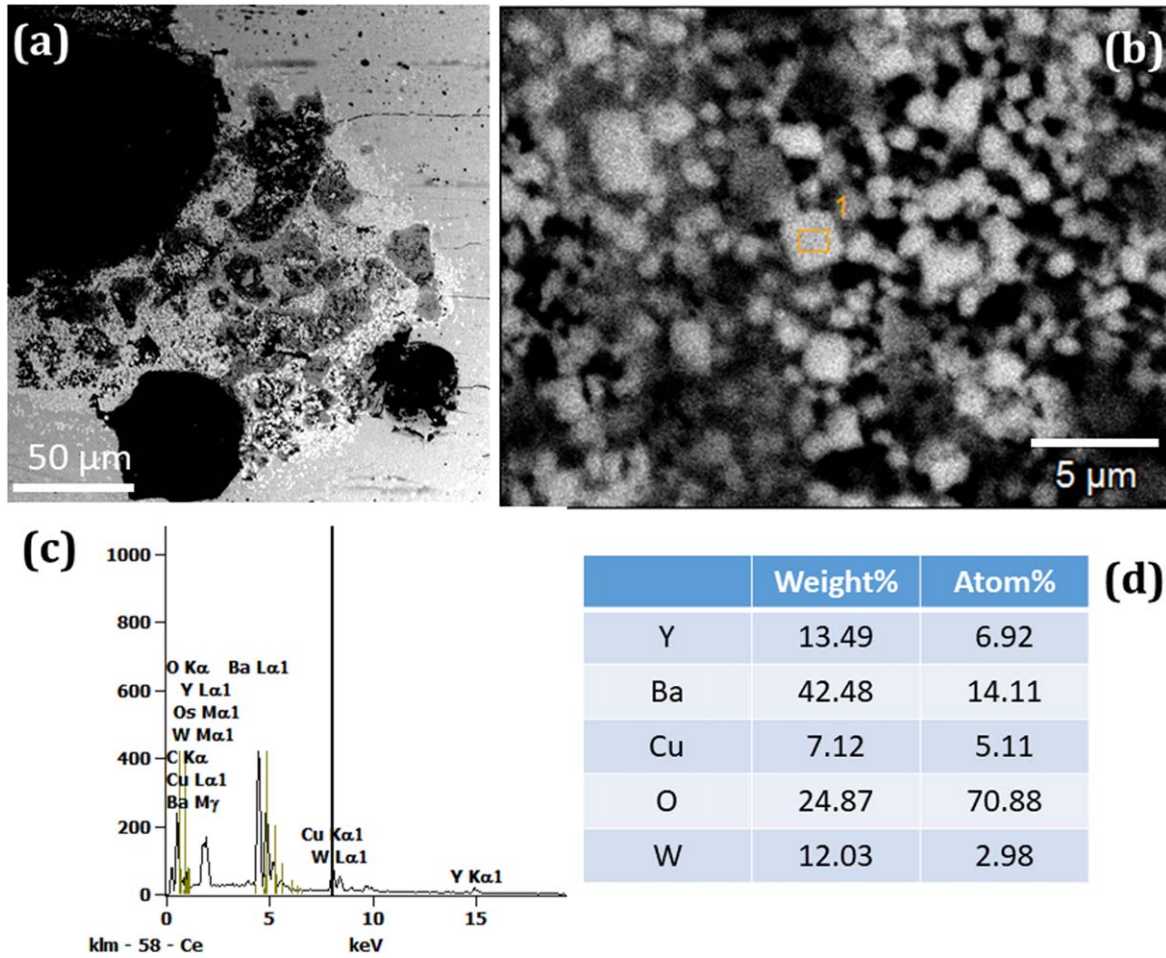
	Weight%	Atom%
Y	13.49	6.92
Ba	42.48	14.11
Cu	7.12	5.11
O	24.87	70.88
W	12.03	2.98

Figure 8. Scanning electron micrographs obtained under different magnifications for the YBCO sample containing W-fibres indicating the formation and presence of the $Y_2Ba_4CuWO_y$ [Y-2411(W)] phase. EDX analysis performed at location '1' in (b) confirmed it to be the Y-2411 phase. (c) EDX data and (d) elemental analysis.
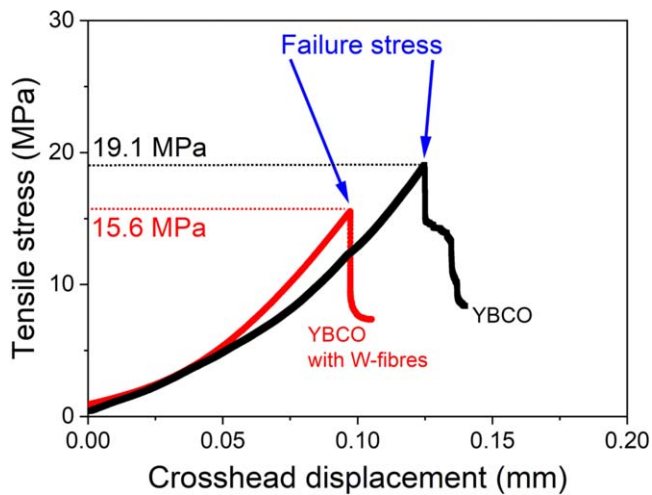

Figure 9. Tensile strength of YBCO samples processed with and without W-fibres measured using the Brazilian technique. It can be seen that the addition of W-fibres reduces the mechanical strength of the YBCO single grain samples.
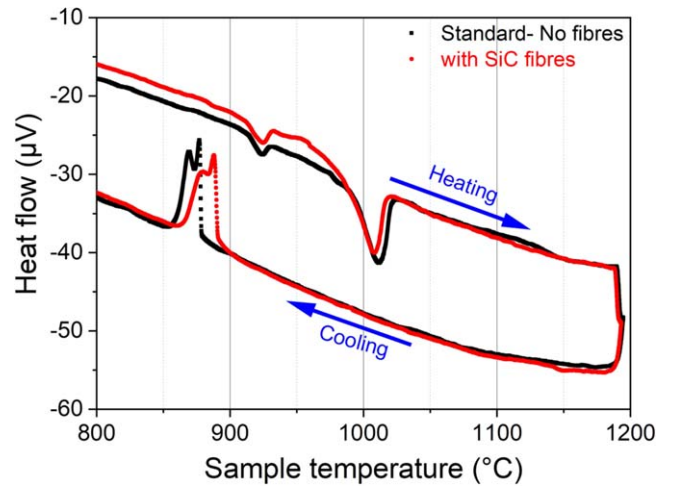
Figure 10. TG-DTA scans obtained for YBCO precursor powder with and without 0.25 wt% SiC fibres. The peritectic temperature is lowered by ~3 °C in the fibre-containing composition compared to the standard powder.

Figure 11. (a) YBCO preform pellet containing dispersed SiC fibres, capped with a buffer pellet and a NdBCO seed crystal prior to BA-TSMG. (b) The sample in (a) grown into a single grain. (c) The trapped field measured at 77 K of the sample shown in (b). The inset in (c) shows the polished surface of the sample above which the trapped field was measured.
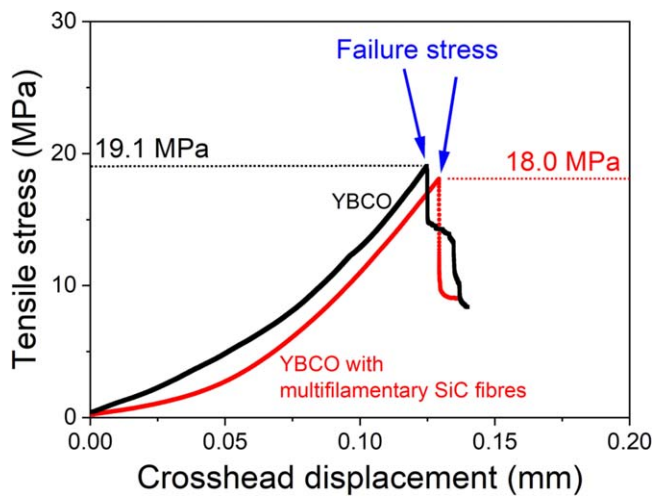

Figure 12. Tensile strength measured employing the Brazilian technique in YBCO samples fabricated with and without dispersed SiC fibres (each of 1.5 micron in diameter). These samples were fabricated employing the BA-TSMG technique.

preforms, the samples were still grown successfully into single grains, as can be seen from figure 13(c). However, the presence of macro-cracks in the single grain fabricated with stacks of fibres in the preform is apparent from the side views of the sample (figure 13(d)), from which it is clear that the fibres have not been dispersed within the precursor powder. The trapped fields measured for samples containing SiC fibre stacks at 77 K are shown in figure 14, which demonstrates that the single grain growth was not compromised by the addition of mutlifilamentary SiC fibres, although mechanical strength of the as-processed single grain did decrease significantly due to the formation of cracks at the interface between the fibres and the YBCO composite.

In both sample configurations, although single grain growth was achieved and a marginal improvement in superconducting properties observed, the mechanical strength of the samples was either almost comparable to that of standard YBCO or had deteriorated due to the formation of additional cracks and pores in the microstructure of the material. It was observed further that the SiC fibres reacted with the liquid phase at elevated temperature, which reduced their strength and reinforcing properties significantly. These

general results and observations provided further motivation to identify an alternative potential fibre that could address the limitations of SiC, as discussed in the following section.

3.3. Mono-filamentary W-SiC fibre reinforced YBCO

A hybrid fibre consisting of a tungsten (W) core of ∼15 μm diameter encapsulated in SiC with an overall diameter of 100 μm was used to reinforce the (RE)BCO RE-123/RE-211 composite. Three of these mono-filamentary hybrid SiC fibres were arranged at the centre of a preform compact, as shown in figure 15(a). Samples containing these fibres were grown successfully in the form of single grains, as can be seen in figure 15(d). No major macro-cracks were observed to form at the center of these samples, unlike those in samples containing non-hybrid multifilamentary SiC fibres (the side views of the samples are shown in figure 15(e)).

The samples containing the hybrid fibres were oxygenated and subsequently machined for measurement of their tensile strength by the Brazilian technique. The measured tensile strength of one of these samples, which is representative of all those measured, is compared with that of a standard YBCO sample in figure 16.

The sample was polished following the mechanical tests and its cross-section observed using a scanning electron microscope. This study revealed good adherence between the fibre and the YBCO matrix, as can be seen in figure 17. It can also be seen that the addition of this hybrid fibre has not resulted in the formation of any unwanted sub-grains or additional grain nucleation, which is critical for retaining the superconducting properties of the single grain samples.

The absence of sub-grain formation as a result of incorporating the hybrid fibres is critical to the retention of good superconducting properties. Additional external reinforcement with stainless steel employing a shrink-fit technique can make the single grain samples sufficiently robust for a variety of high field applications, such as motors and bearings where these materials can be subjected to large rotational forces and bursting stress.

The incorporation of hybrid fibres is also possible in other YBCO growth processes. Figure 18 shows single grain YBCO samples grown via top-seeded infiltration growth (TSIG) route [34–36] containing reinforcing fibres.
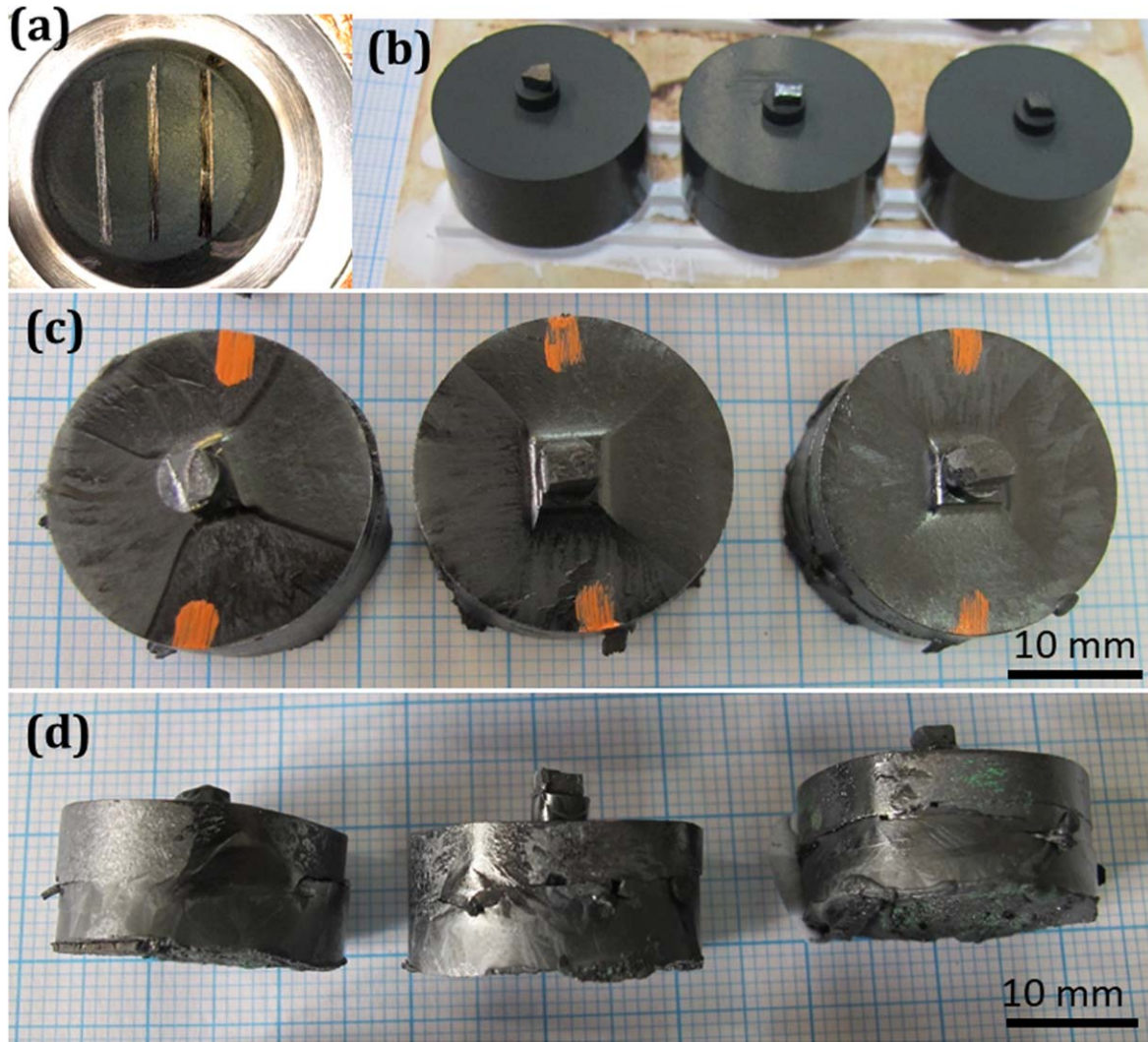
Figure 13. (a) The position of three multifilament SiC fibre stacks at the centre of the preform compact. (b) Sample assemblies comprising of the preform containing fibres, capped with buffer pellet and a seed crystal. The top and side views of the grown single grained YBCO samples containing these multifilamentary SiC fibres are shown in (c) and (d), respectively.
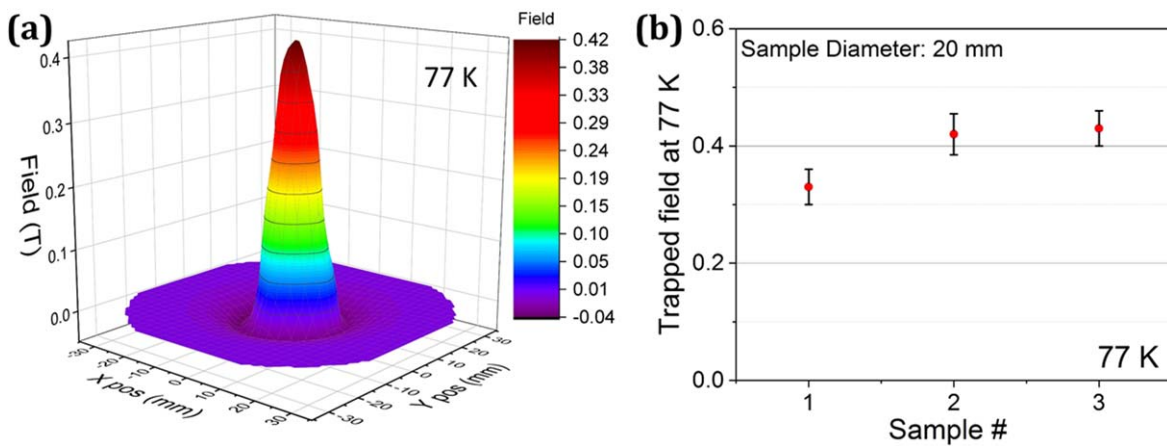

Figure 14. (a) Typical trapped field profile measured at 77 K for the YBCO sample containing multifilamentary SiC fibres at the center of the preform compact. (b) Peak trapped field measured in three samples fabricated employing a similar methodology.
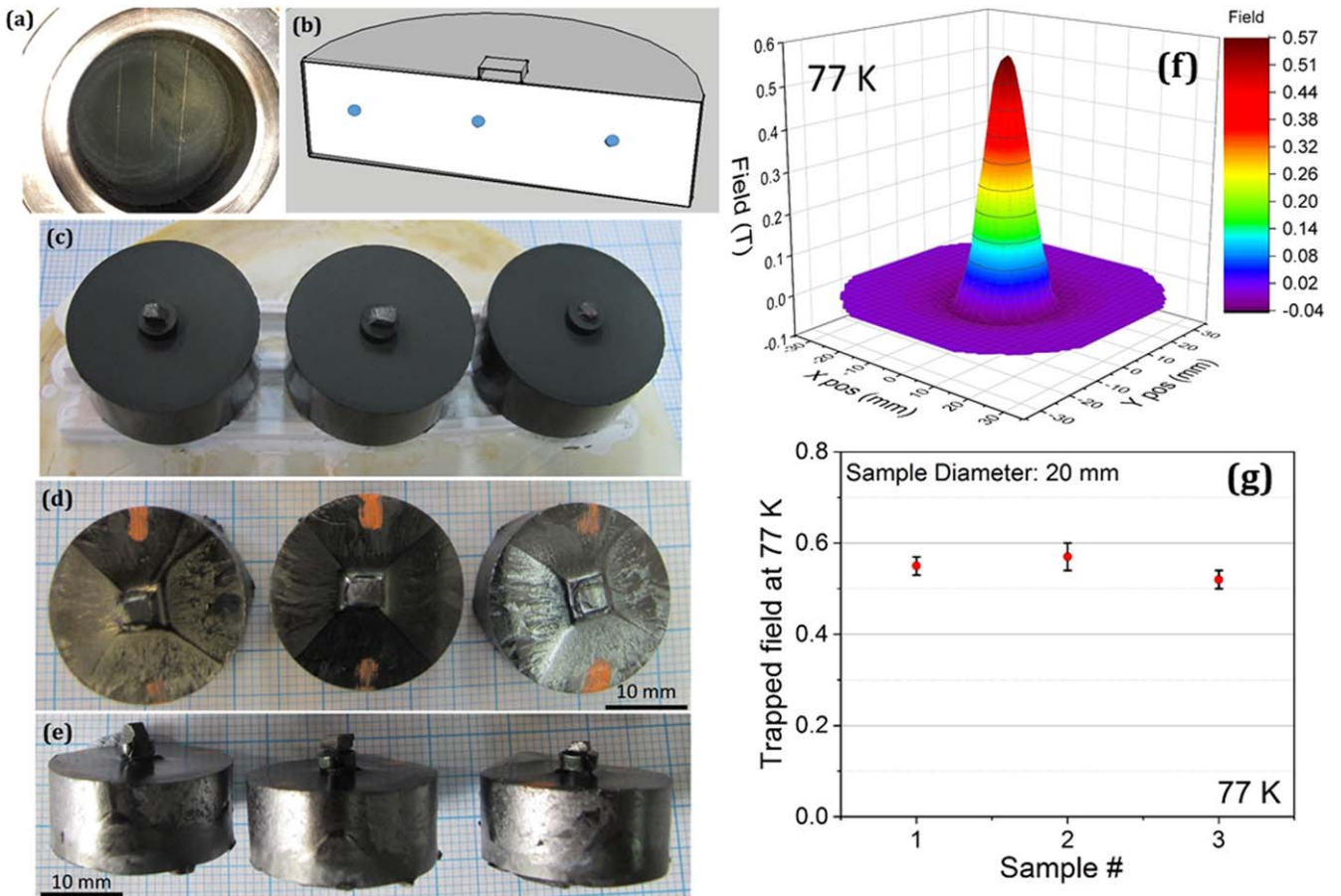
Figure 15. (a) Photograph showing the position of three mono-filament hybrid SiC fibres directly within the precursor powder within the steel die at the center of the preform compact (i.e. prior to the addition of the remaining precursor powder) and illustrated schematically in (b). (c) Three sample assemblies prepared with hybrid fibres. (d) and (e) Fully processed single-grain samples in top and side elevation, respectively. (f) Trapped field measured at 77 K for one of these samples and (g) peak field measured for all three samples.
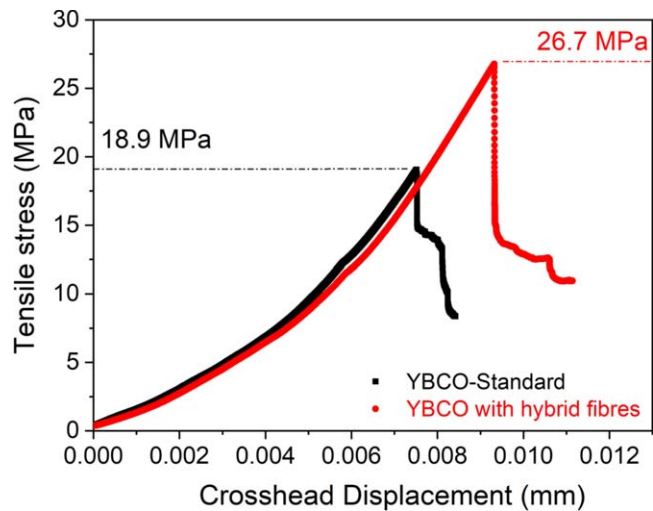

Figure 16. Tensile strength measured for single grain YBCO samples fabricated with and without embedded mono-filament hybrid SiC fibres containing a W-core.

Figure 17. Cross-section of the YBCO sample containing mono-filament hybrid SiC fibres. The micrograph shows that the fibres exhibit good adherence within the YBCO matrix and that their presence does not affect the single grain growth process.

3.4. Phase stability test—results

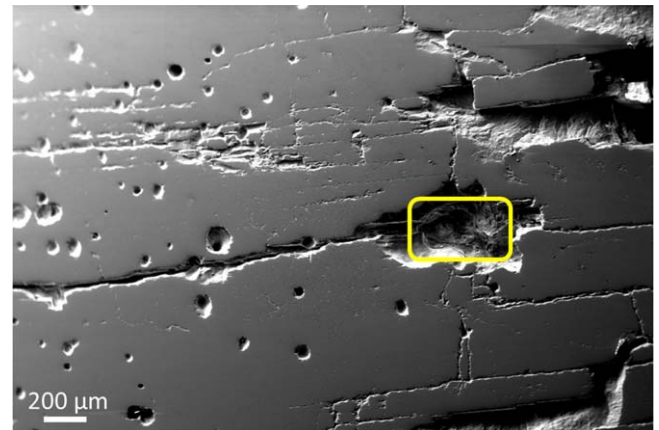The phase stability of the W, mutifilamentary SiC and hybrid SiC fibres used in the present work was investigated by examining the microstructures of the as-grown, single grain YBCO samples. Optical micrographs obtained under both low and high magnification are shown figures 19(b)–(g). It can be seen that both W and multifilamentary SiC fibres have undergone reactions with the liquid phase and have
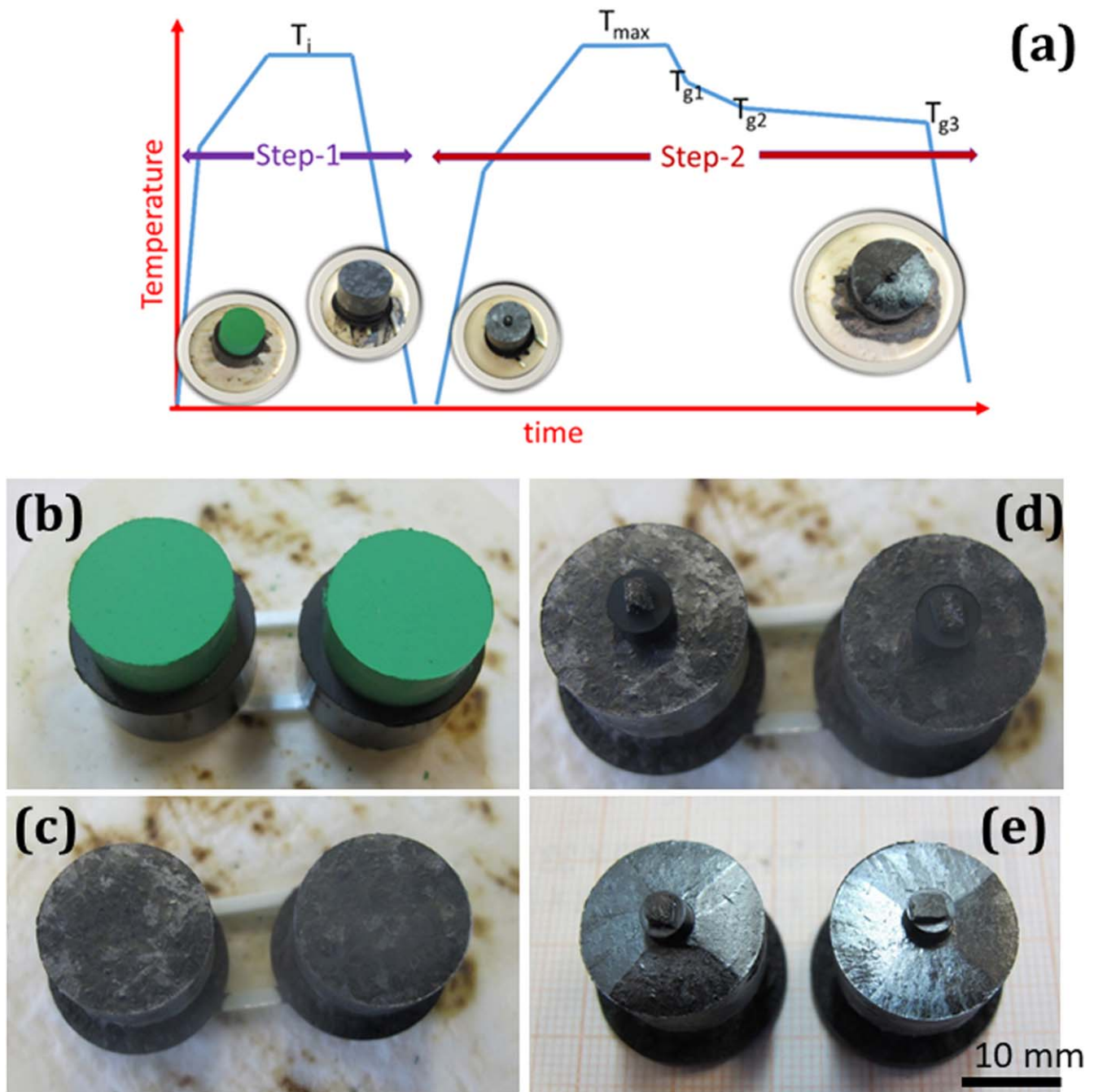
Figure 18. (a) YBCO samples containing hybrid SiC fibres fabricated by a 2-step buffer-aided TSIG process and a schematic illustration of the 2-step TSIG fabrication process. (b)–(e) Various stages of the infiltration and growth process.

disintegrated either partially or completely in the YBCO phase matrix, whereas hybrid SiC fibres containing W in the core retain their physical characteristics, as is evident from figures 19(e) to (g). Furthermore, the resilience of these hybrid SiC fibres can be seen in the scanning electron micrographs shown in figures 19(h) and (i). The EDX analysis carried out on these samples confirmed that the central location (white in contrast in figure 19(i)) corresponds to W and the surrounding area to SiC, establishing clearly that this fibre integrates well into the matrix whilst simultaneously retaining its physical structure.

These observations suggest clearly that SiC does not have any appreciable chemical interaction with the components of the bulk superconductors fabricated in this study. Furthermore, hybrid mono-filamentary SiC fibres have been introduced to the single grain to successfully reinforce the (RE)BCO bulk microstructure and, as a result, to improve the tensile strength of these ceramic-like materials by up to ∼40%. It may be concluded, therefore, that single grain YBCO reinforced with hybrid mono-filamentary SiC fibres have significant potential for a new generation of high field engineering applications.
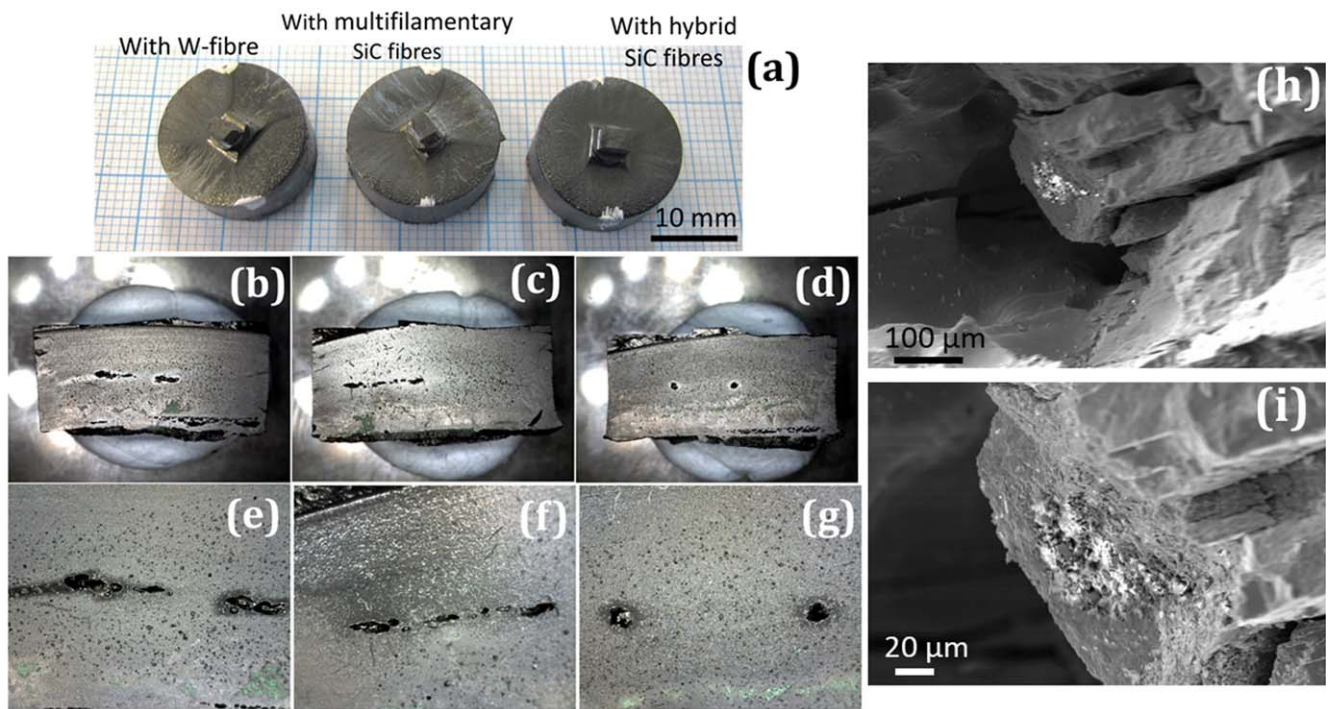
Figure 19. (a) Photographs obtained for YBCO samples containing fibres (W, multifilamentary SiC and hybrid SiC). Optical micrographs obtained from the cross-sections of these samples under low and high magnifications are shown in (b)–(d) and (e)–(g), respectively. Scanning electron micrographs obtained in the vicinity of the hybrid fibre location in the single-grain YBCO sample are shown in (h) and (i).

4. Conclusions

The reinforcement of single grain, (RE)BCO bulk superconductors fabricated by TSMG via the use of tungsten-cored SiC hybrid fibres has produced a significant improvement in the tensile strength of these technologically important materials. Critically, we have demonstrated that SiC does not react with the superconducting matrix during processing at elevated temperatures and is thermally stable, meaning that this is both a practical and effective reinforcement technique. The key advantage of the approach described here is that the fibres are introduced to the precursor at an early stage of sample growth, which makes the application of the fully processed material more straightforward than competing approaches based on external reinforcement. However, it may prove to be the case that further progress towards the prospect of generating trapped magnetic fields in excess of 20 T, as predicted theoretically, is achieved via the use of a combination of internal reinforcement, as discussed here, and those developed previously using external reinforcement techniques.

ORCID iDs

Devendra K Namburi ⓘ https://orcid.org/0000-0003-3219-2708
Kaiyuan Huang ⓘ https://orcid.org/0000-0001-7476-305X
Yunhua Shi ⓘ https://orcid.org/0000-0003-4240-5543
David A Cardwell ⓘ https://orcid.org/0000-0002-2020-2131
John H Durrell ⓘ https://orcid.org/0000-0003-0712-3102

References

[1] Cardwell D A 1998 Processing and properties of large grain (RE)BCO *Mater. Sci. Eng.* B **53** 1–10
[2] Cloots R, Koutzarova T, Mathieu J-P and Ausloos M 2005 From RE-211 to RE-123. How to control the final microstructure of superconducting single-domains *Supercond. Sci. Technol.* **18** R9–23
[3] Sakai N, Kita M, Nariki S, Muralidhar M, Inoue K, Hirabayashi I and Murakami M 2006 Field trapping property of Gd–Ba–Cu–O bulk superconductor 140 mm in diameter *Physica* C **445–448** 339–42
[4] Murakami M 1993 Novel application of high T_c bulk superconductors *Appl. Supercond.* **1** 1157–73
[5] Campbell A M and Cardwell D A 1997 Bulk high temperature superconductors for magnet applications *Cryogenics* **37** 567

[6] Jin S, Tiefel T H, Sherwood R C, van Dover R B, Davis M E, Kammlott G W and Fastnacht R A 1998 Melt-textured growth of polycrystalline YBa$_2$Cu$_3$O$_{7-\delta}$ with high transport J_c at 77 K *Phys. Rev.* B **37** 7850–3

[7] Jee Y A, Kim C-J, Sung T-H and Hong G-W 2000 Top-seeded melt growth of Y–Ba–Cu–O superconductor with multiseeding *Supercond. Sci. Technol.* **13** 195

[8] Cardwell D A, Shi Y-H, Hari Babu N, Pathak S K, Dennis A R and Iida K 2010 Top seeded melt growth of Gd–Ba–Cu–O single grain superconductors *Supercond. Sci. Technol.* **23** 034008

[9] Nariki S, Sakai N and Murakami M 2005 Melt-processed Gd–Ba–Cu–O superconductor with trapped field of 3 T at 77 K *Supercond. Sci. Technol.* **18** S126

[10] Hari Babu N, Reddy E S, Cardwell D A and Campbell A M 2003 Artificial flux pinning centers in large, single-grain (RE)–Ba–Cu–O superconductors *Appl. Phys. Lett.* **83** 4806

[11] Muralidhar M, Jirsa M, Sakai N and Murakami M 2003 Progress in melt-processed (Nd Sm Gd)Ba$_2$Cu$_3$O$_y$ superconductors *Supercond. Sci. Technol.* **16** R1–16

[12] Tomita M and Murakami M 2003 High-temperature superconductor bulk magnets that can trap magnetic fields of over 17 tesla at 29 K *Nature* **421** 517–20

[13] Durrell J H, Dennis A R, Jaroszynski J, Ainslie M D, Palmer K G, Shi Y and Cardwell D A 2014 A trapped field of 17.6 T in melt-processed, bulk Gd–Ba–Cu–O reinforced with shrink-fit steel *Supercond. Sci. Technol.* **27** 082001

[14] Johansen T H 2000 Flux-pinning-induced stress and magnetostriction in bulk superconductors *Supercond. Sci. Technol.* **13** R121–37

[15] Ren Y, Weinstein R, Liu J, Sawh R P and Foster C 1995 Damage caused by magnetic pressure at high trapped field in quasi-permanent magnets composed of melt-textured Y–Ba–Cu–O superconductor *Physica* C **251** 15–26

[16] Fuchs G, Schätzle P, Krabbes G, Gruß S, Verges P, Müller K-H, Fink J and Schultz L 2000 Trapped magnetic fields larger than 14 T in bulk YBa$_2$Cu$_3$O$_{7-x}$ *Appl. Phys. Lett.* **76** 2107

[17] Zhou Y-H and Yong H-D 2007 Crack problem for a long rectangular slab of superconductor under an electromagnetic force *Phys. Rev.* B **76** 094523

[18] Schatzle P, Krabbes G, Grub S and Fuchs G 1999 YBCO/Ag bulk material by melt crystallization for cryomagnetic applications *IEEE Trans. Appl. Supercond.* **9** 2022–5

[19] Devendra Kumar N, Rajasekharan T and Seshubai V 2011 YBCO/Ag composites through a preform optimized infiltration and growth process yield high current densities *Supercond. Sci. Technol.* **24** 085005

[20] Congreve J V J, Shi Y, Dennis A R, Durrell J H and Cardwell D A 2018 The successful incorporation of Ag into single grain, Y–Ba–Cu–O bulk superconductors *Supercond. Sci. Technol.* **31** 035008

[21] McDanels D L 1985 Analysis of stress-strain, fracture, and ductility behavior of aluminum matrix composites containing discontinuous silicon carbide reinforcement *Metall. Trans.* A **16** 1105–15

[22] Nozawa T *et al* 2009 Recent advances and issues in development of silicon carbide composites for fusion applications *J. Nucl. Mater.* **386–388** 622–7

[23] Yu X-M, Zhou W-C, Luo F, Zheng W-J and Zhu D-M 2009 Effect of fabrication atmosphere on dielectric properties of SiC/SiC composites *J. Alloys Comp.* **479** L1–3

[24] Sarkar S and Das P K 2014 Effect of sintering temperature and nanotube concentration on microstructure and properties of carbon nanotube/alumina nanocomposites *Ceram. Int.* **40** 7449–58

[25] Tu W-C, Lange F F and Evans A G 1996 Concept for a damage-tolerant ceramic composite with 'strong' interfaces *J. Amer. Ceram. Soc.* **79** 417–24

[26] Shi Y, Hari Babu N and Cardwell D A 2005 Development of a generic seed crystal for the fabrication of large grain (RE)–Ba–Cu–O bulk superconductors *Supercond. Sci. Technol.* **18** L13

[27] Namburi D K, Shi Y, Dennis A R, Durrell J H and Cardwell D A 2018 A robust seeding technique for the growth of single grain (RE)BCO and (RE)BCO–Ag bulk superconductors *Supercond. Sci. Technol.* **31** 044003

[28] Devendra Kumar N, Shi Y-H, Zhai W, Dennis A R, Durrell J H and Cardwell D A 2015 Buffer Pellets for high-yield, top-seeded melt growth of large grain Y–Ba–Cu–O superconductors *Cryst. Growth Des.* **15** 1472–80

[29] Withnell T D, Hari Babu N, Ganney I, Dennis A and Cardwell D A 2008 High-field flux mapping of (RE)BCO bulk superconductors-development of an *in situ* scanning system *Mater. Sci. Eng.* B **151** 79–83

[30] Fairhurst C 1964 On the validity of the 'Brazilian' test for brittle materials *Int. J. Rock Mech. Min. Sci. Geomech.* **1** 535–446

[31] Andreev G E 1991 A review of the Brazilian test for rock tensile strength determination *Min. Sci. Technol.* **13** 445–56

[32] Huang K Y *et al* 2018 Spatial distribution of flexural strength in Y–Ba–Cu–O bulk superconductors *IEEE Trans. Appl. Supercond.* **28** 6801505

[33] Hari Babu N, Iida K and Cardwell D A 2006 Enhanced magnetic flux pinning in nano-composite Y–Ba–Cu–O superconductors *Physica* C **445–448** 353

[34] Namburi D K, Shi Y-H, Palmer K G, Dennis A R, Durrell J H and Cardwell D A 2016 A novel, two-step top seeded infiltration and growth process for the fabrication of single grain, bulk (RE)BCO superconductors *Supercond. Sci. Technol.* **29** 095010

[35] Noudem J G, Meslin S, Hovarth D, Harnois C, Chateigner D, Ouladdiaf B, Eve S, Gomina M, Chaud X and Murakami M 2007 Infiltration and top seed growth-textured YBCO bulks with multiple holes *J. Am. Ceram. Soc.* **90** 2784–90

[36] Diko P, Vojtkova L, Vojtko M and Rajnak M 2019 Microstructural aspects of infiltration growth YBCO bulks with chemical pinning *IEEE Trans. Appl. Supercond.* **29** 6800805